NUWC-NL Technical Document 10,001
28 February 1992

Scatter Channels and Target Modeling for Active Signal Extraction in Underwater Acoustics: II. Summary and Synthesis of I, [1].

Antisubmarine Warfare Systems Department

Naval Undersea Warfare Center
Detachment, New London, Connecticut

PREFACE

This document was prepared for the ASW Systems Department by Dr. David Middleton of Sonalysts, Inc. under Contract N66604-91-D-0091-008 under the direction of Dr. Duncan Sheldon (Code 3314).

The technical reviewers for this report were Mr. R. W. Read (Code 331) and Mr. R. O. Barton (Code 3314).

REVIEWED AND APPROVED: 28 FEBRUARY 1992

D. W. COUNSELLOR
Head, Antisubmarine Warfare Systems Department

Unclassified
SECURITY CLASSIFICATION OF THIS PAGE

REPORT DOCUMENTATION PAGE

1a. REPORT SECURITY CLASSIFICATION Unclassified	1b. RESTRICTIVE MARKINGS
2a. SECURITY CLASSIFICATION AUTHORITY	3. DISTRIBUTION/AVAILABILITY OF REPORT Approved for public release; distribution unlimited
2b. DECLASSIFICATION/DOWNGRADING SCHEDULE	
4. PERFORMING ORGANIZATION REPORT NUMBER(S) TD-10,001	5. MONITORING ORGANIZATION REPORT NUMBER(S)
6a. NAME OF PERFORMING ORGANIZATION Naval Undersea Warfare Center 6b. OFFICE SYMBOL (If applicable) Code 3314	7a. NAME OF MONITORING ORGANIZATION
6c. ADDRESS (City, State, and ZIP Code) Detachment, New London New London, CT 06320	7b. ADDRESS (City, State, and ZIP Code)
8a. NAME OF FUNDING/SPONSORING ORGANIZATION 8b. OFFICE SYMBOL (If applicable)	9. PROCUREMENT INSTRUMENT IDENTIFICATION NUMBER
8c. ADDRESS (City, State, and ZIP Code)	10. SOURCE OF FUNDING NUMBERS PROGRAM ELEMENT NO. / PROJECT NO. / TASK NO. / WORK UNIT ACCESSION NO.

11. TITLE (Include Security Classification)

Scatter Channels and Target Modeling for active Signal Extraction in Underwater Acoustics: II. Summary and Synthesis

12. PERSONAL AUTHOR(S)
David Middleton

13a. TYPE OF REPORT	13b. TIME COVERED	14. DATE OF REPORT (Year, Month, Day)	15. PAGE COUNT
Tech. Document	FROM 5/91 TO 9/91	92 Feb 28	30

16. SUPPLEMENTARY NOTIFICATION
See Glossary of Principal Symbols

17. COSATI CODES		
FIELD	GROUP	SUB-GROUP

18. SUBJECT TERMS (Continue on reverse if necessary and identify by block number)
Acoustic Target Detection: scatter channels, WSSUS channels; channel as linear filter; threshold detection; detection performance; analytic channel and target models; signal design.

19. ABSTRACT (Continue on reverse if necessary and identify by block number)

The purpose of this document is to provide a review and synthesis of the author's recent detailed analyses of scatter channels and target models for the active threshold detection of underwater targets in an ocean environment [1]. The summary and synthesis describe the main results of analytic modeling of: (1) Generalized scatter (reverberation) channels; (2) Line target models, with bistatic orientation and doppler; (3) Threshold detection algorithms for the mixed gauss, non-gauss ambient and reverberation noise; (4) The detection parameter governing performance for these dominant signal-dependent noise milieux. In addition to the general canonical treatment, the results provide a framework for signal (i.e., waveform) design to maximize further the expected performance. A short list of next steps in the analytic program is included, along with selected references.

20. DISTRIBUTION/AVAILABILITY OF ABSTRACT	21. ABSTRACT SECURITY CLASSIFICATION	
☒ UNCLASSIFIED/UNLIMITED ☒ SAME AS RPT. ☐ DTIC USERS	Unclassified	
22a. NAME OF RESPONSIBLE INDIVIDUAL Dr. Duncan Sheldon	22b. TELEPHONE (Include Area Code) 203-440-5486	22c. OFFICE SYMBOL

DD FORM 1473, 84 MAR

83 APR edition may be used until exhausted.
All other editions are obsolete.

SECURITY CLASSIFICATION OF THIS PAGE
Unclassified

Table of Contents

List of Figures

Glossary of Principal Symbols

A_o = peak signal amplitude

$A_1^{(o)}$, $A_2^{(1)}$, $A_2^{(k)}$ = average numbers of scatterers

$\mathcal{A}_T$, $\mathcal{A}_R$, $\mathcal{A}_{RT}$ = (complex) beam patterns

α = scalar (acoustic) field

α_H, α_S = homogeneous, scatter fields

a = absorption constant

$a_{o\text{-}min}^{(*)}$ = min. detectable signal

$\hat{B}_J$, $\hat{B}^{(o)}$ = bias in detection algorithm

$\otimes$ = convolution

c = speed of propagation

χ, χ_o = ambiguity functions

∇^2 = Laplacian

∇ = gradient operator

δ = (Dirac) delta function

ε_o, ε, $\hat{\varepsilon}$ = epochs

$\hat{\eta}$, $\hat{\eta}_\infty$ = field renormalization operators

η_o = fading parameter

$F_{S,AB}$ = reverberation structure factors

F_1 = characteristic function (c.f.)

$\mathcal{F}$, $\mathcal{F}^{-1}$ = Fourier transforms

F_L, f_L = TSFT: total spreading functions of target

$G^{(1)}$ = "geometric factor"

$\hat{G}_T$ = source operator

G_A, G_T = source function, ambient and input signal

g_∞, $g^{(Q)}$ = green's functions

g_J^* = detection algorithm

$\mathcal{G}_A$ = ambient noise source function

γ_o, γ_{o1} = scatterer cross-section

H_0, H_1 = hypothesis states

$h_{T,R}$ = weighting functions

h_s, h_A = filter operators

h_M = matched filter

I_X = intensity of X

$\hat{\mathbf{i}}_l$, $\hat{\mathbf{i}}_{oT}$, $\hat{\mathbf{i}}_{oR}$, $\hat{\mathbf{i}}_x$, $\hat{\mathbf{i}}_y$, $\hat{\mathbf{i}}_z$ = unit vectors

J = space-time sample size = MN

$|J|$ = |jacobian|

J_o = Bessel function, first kind, zero order

$K_X^{(1)}$, K_X, K, K_{dN}, k_o, $k_o^{(1)}$, k_T = covariances

$\mathbf{k}_o$ = vector wave number

$L^{(2)}$ = statistic of (nongaussian) noise

$l(x)$ = transfer function of threshold detector

Λ_J = likelihood ratio

$\hat{L}^{(0)}$, $\hat{L}^{(1)}$ = propagation operators

λ, Λ_S = coördinate, region

l = unit length in space

l_x, l_y, l_z = direction cosines

$\hat{M}^{(Q)}$, $\hat{M}$, $\hat{M}_\infty$ = integral green's function operators

$M_{X-<X>}$, M_X, $M_{<X>}$ = second-moment functions of X, <X>

μ = ratio of *a priori* probabilities

N_A = ambient noise
N = total number
N(S) = signal-dependent noise
$\nu(Z)$ = density of scatterers
ν = frequency spread
$\hat{N} = \int(\ )dN(Z)$ = counting functional
dn, dN = numbers of scatterers

Ω_s = cospreading function of scatter channel
ω_o = carrier angular frequency

Ψ = noise intensity
P(R,t) = point in field
P_D = prob. of detection
$\Pi^{(*)}$ = processing gain

$\hat{Q}$ = inhomogeneity operator
q_L = target scatter kernel

R_{oT}, R_{oR} = distances
$\hat{R}$ = receiving array operator
Re = real part of
ρ_o = process density

S_{in} = input signal
σ_J^* = detection parameter

σ_S = scattering function
$s_o(t)$, $\hat{s}_o$ = normalized n.b. signal waveforms
S_L = received target signal

T_{AR}, $T_T^{(N)}$, T_{AT} = channel and coupling operators
$T_o(\lambda)$ = path delay
T = observation interval, signal duration
Θ = error function
τ = path delay; t_2–t_1; etc.
θ, θ_{min} = normalized received signals

U, U_j, U_o = basic waveforms

v_D = doppler speed

$\mathcal{W}$ = intensity spectrum

X(t), $X_s(t)$ = received waveforms
X, **x** = received data vectors

$Y_m(t)$ = output of m-th sensor element

Z, Z_R, Z_θ, Z_s = random variables, domains
ζ = surface elevation

Principal Acronyms and Abbreviations

AWGN	= additive "white" gaussian noise
AWnonGN	= additive "white" nongaussian noise
GHP	= generalized Huyghens Principle
LOB	= locally optimum Bayes
MFP	= matched field processing; (global, cf. [18], [19])
PTSS	= perturbation theoretical series solution
RSF	= reverberation structure factor
SS	= single scatter
TSF	= target structure factor
TSFT	= total spreading function of target
WSSUS	= wide sense stationary uncorrelated scatter
ZMNL	= zero-memory nonlinear
c.f.	= characteristic function
f.f.	= far-field
n.b.	= narrow band
N.B.	= narrow beam
s.d.	= small doppler

Scatter Channels and Target Modeling For Active Signal Extraction in Underwater Acoustics: II. (Summary and Synthesis of I, [1])

by David Middleton*

August 1991

SECTION 1. INTRODUCTION

The main purpose of the document is to provide a concise review and synthesis of the detailed analytic models described in current work of the author [1] directed toward the active acoustic detection of underwater targets in the ocean. The aims here are primarily descriptive and summarial, with the emphasis on motivation and interpretation rather than on the analytic details which are developed in [1] itself and which follow from earlier studies [2]. Of course, an analytic structure of sufficient sophistication is required in technical applications and for the quantitative guidance of experiment. In our review we shall for the most part provide the main results from [1] and show how they are important in obtaining effective detection of underwater acoustic targets. Here, we are concerned principally with (i), weak narrowband signals in the far-field, and (ii) dominant signal-dependent noise or reverberation, since these are usually the critical limiting factors in performance.

The principal model components may be identified typically as follows:

I. The generalized channel model, expressed in terms of (linear) spatio-temporal filters and consisting of both scatter (reverberation) and ambient noise mechanisms and including the array coupling at source and receiver;

II. Target models, which should be analytically simple but still retain the principal features of typical targets, e.g., cross-section, specular and diffuse scattering mechanisms, spatial distribution, and Doppler;

III. Statistical-physical descriptions of the ambient and scatter components of the channel, and the target, e.g., moments, covariances, and pdf's, as needed for the signal processing required in IV ff; and

IV. Detection algorithms and performance, whose parameters are determined by the model elements of I-III, and which incorporate both the geometry and propagation features of source, target, and the medium explicitly.

Although the present approach includes nongaussian noise components, it is for the moment analytically limited to iso-velocity propagation conditions, where $\nabla c = 0$. The quantitative extension to the more realistic geometries implied by $\nabla c \neq 0$, namely first-to-third convergence zone (CVZ) applications, is one of the suggested next steps in extending the analysis. However, the assumption $\nabla c = 0$ here in no way destroys the canonical nature of the results or the generality of the methods employed.

---

* 127 East 91st Street; New York, NY 10128.

The organization of this paper follows closely the topical outline of I-IV above, with a short summary of the principal results and needed next steps in the analysis and suggested experimental efforts.

SECTION 2. THE CANONICAL CHANNEL AS A LINEAR FILTER

The canonical channel is shown schematically in *Figure 2.1*. It is postulated to be linear, but is otherwise unrestricted. This structure suggests that it can be represented equivalently by a spatio-temporal linear filter that is generally time- and space-variable with a variety of injected noise sources, in the manner of *Figure 2.2* below, where $h_S(= h_R + h_D)$ is the weighting or green's function of the medium, excluding the coupling operations $h_{T,Rc}$. Here h_R and h_D are respectively the random and deterministic components of $h_S = h_S(\mathbf{R}', \mathbf{R}|\tau, t)$.

The quantities $h_{T,}R_C(\sim\mathcal{A}_{T,R})$ in *Figure 2.1* represent the coupling to the medium (T = source; Rc = receiver), with $\mathcal{A}_{T,R}$ the beam patterns associated with the filters ($h_{T,R}$) of these coupling apertures. Here also, $S_{in} = S_{in}(t)$ is the original (encoded) input signal, and $\hat{G}_T$ is the aperture operator, such that (Sec. II [2] the input signal source function G_T, becomes

$$G_T(t,\xi) \equiv \hat{G}_T S_{in} = \int_{-\infty}^{\infty} h_T(t-\tau|\xi) S_{in}(\tau,\xi) d\tau \,, \tag{2.1}$$

where in general h_T is treated as time-variable, because of possible motion of the source.

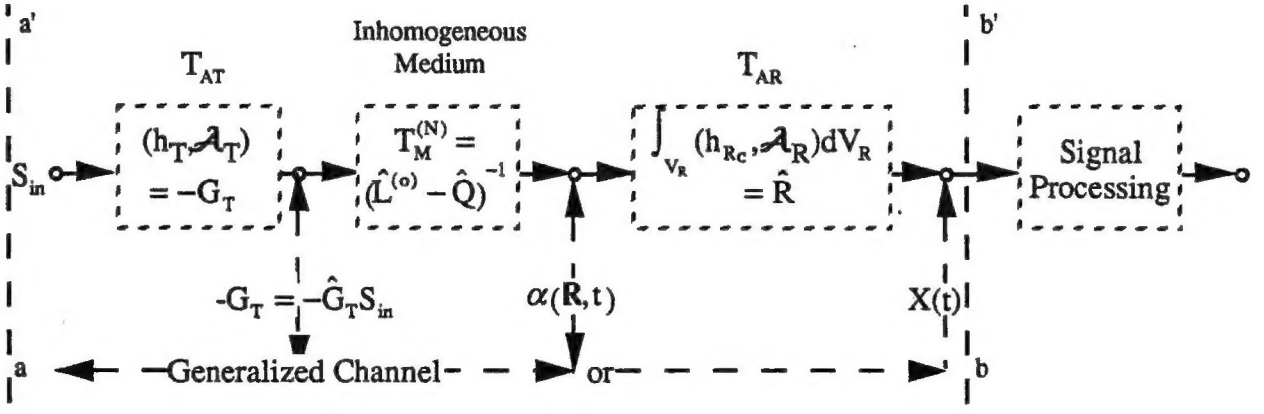

Figure 2.1 Operational schematic of an inhomogeneous linear medium, with source and receiver coupling. Here $\hat{Q}$ is the inhomogeneity operator associated with this general, inhomogeneous linear medium.

Similarly, X(t) is the output of the receiving aperture, expressed by the operator $\hat{R}$, e.g.,

$$X(t) = \hat{R}\alpha(\mathbf{R}, t) = \int_{V_R} dV_R(\mathbf{R}) \int_{-\infty}^{\infty} h_{Rc}|(t-\tau, t|\mathbf{R} \in V_R)\alpha(\mathbf{R}, \tau) d\tau \tag{2.2}$$

where h_{Rc} ($\neq h_R$ above) is possibly time-variable also. Here $\alpha(\mathbf{R},t)$ is the field propagated in the medium, due to ambient and injected signal sources (S_{in}). Note that both the transmitting and receiving apertures, or arrays, are generally frequency selective: only for suitably narrowband signals vis-à-vis these apertures can the latter be treated as essentially frequency insensitive, an approximation used throughout this study.

2.1 Channel Operators and Filter Equivalents:

The various channel operators of *Figure 2.1* are represented by

$$\mathbf{T}_{AR} = \hat{R}\,\mathbf{T}_{AT} = -\hat{G}_T - \hat{G}_A, \tag{2.3a}$$

where $\hat{G}_A$ is associated with ambient noise in the medium (Sec. 2.1 of [1]), and that of the medium itself is given by the operator relation (Sec. 2, [1]).

$$\mathbf{T}_M^{(N)} = (\hat{L}^{(0)} - \hat{Q})^{-1}, \tag{2.3b}$$

where the general field $\alpha(\mathbf{R},t)$ is formally found from

$$\left(\hat{L}^{(0)} - \hat{Q}\right)\alpha = -G_T - G_A, \text{ with } \left(\hat{L}^{(0)} - \hat{Q}\right)g^{(Q)} = -\delta_{tt'}\delta_{\mathbf{RR}'}, \tag{2.4}$$

in which $g^{(Q)}$ is the green's function of the medium, including boundaries and G_A is the local (space-time) source functions of the ambient field. The $\hat{L}^{(0)} - \hat{Q}$ represents the propagation operators. For example, for an inhomogeneous medium obeying a Helmholtz wave equation, one can write (in rectangular coördinates: $\mathbf{R} = \hat{i}_x x + \hat{i}_y y + \hat{i}_z z$):

$$\left(\nabla^2 - \frac{1}{c_o^2}(1+\epsilon[\mathbf{R},t])\frac{\partial^2}{\partial t^2}\right)\alpha = -(G_T + G_A), \text{ or } = 0, \text{ outside source domains,} \tag{2.5a}$$

with

$$\therefore\ \hat{L}^{(0)} \equiv \nabla^2 - \frac{1}{c_o^2}\frac{\partial^2}{\partial t^2}\ ;\ \hat{Q} \equiv \frac{1}{c_o^2}\epsilon(\mathbf{R},t)\frac{\partial^2}{\partial t^2} \tag{2.5b}$$

for a particular representation of the medium. The homogeneous part is described by $\hat{L}^{(0)}$, while the inhomogeneous effects are represented by $\hat{Q}$. Of course, the medium from our viewpoint is random, so that properly $\hat{Q}$ is a random operator (with ϵ is (2.5b) a random *field*). Equations (2.4), (2.5) embody an *ensemble* of representations, which is called a *Langevin Equation*, whose solutions are *statistics* of the random field α. [See [2], Part I; also, Chapter 10 of [3].] It is these statistics, particularly the lower order moments, which we shall need to describe the effects of the generalized channel on our transmitted and received signals here, contained in X(t), (2.2).

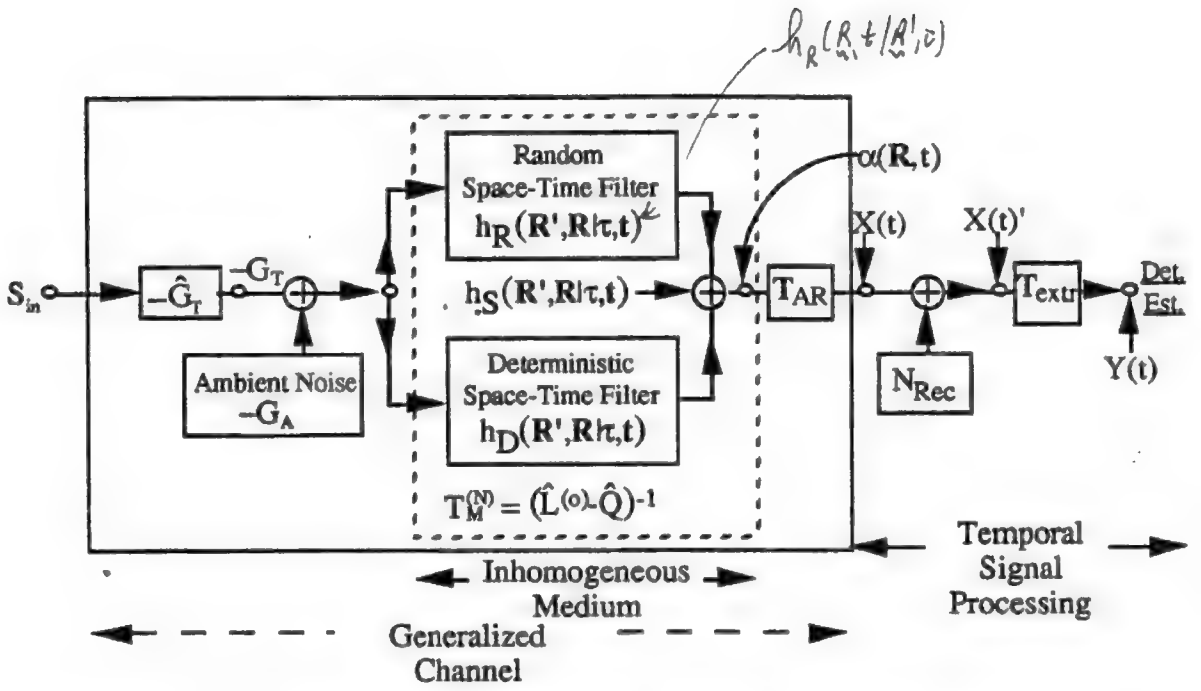

Figure 2.2 Generalized linear inhomogeneous channel, showing ambient noise mechanisms, scattering operations, and coupling, for input signal S_{in} and (temporal) receiver processing for detection and/or estimation. The random and deterministic components of the medium are indicated.

The space-time (now random) filter equivalent to the random inhomogeneous medium is schematically presented in *Figure 2.2*, which is the "filter" form of *Figure 2.1* above. The green's function or "impulse response" of this inhomogeneous medium is indicated by

$$h_S(\mathbf{R}',\mathbf{R}|\tau,t) \equiv g^{(Q)}(\mathbf{R},t|\mathbf{R}',\tau) = g_R^{(Q)} + g_D^{(Q)} , \qquad (2.6)$$

with $g_R^{(Q)}$, $g_D^{(Q)}$ respectively the random and deterministic parts of $g^{(Q)}$. A major task of all investigations of such media is to determine $g^{(Q)}$, or reasonable approximations, and the associated statistics. The results of this must then be applied to the various noise (reverberation) and signal models, from which in turn the desired detection algorithms and system performance are to be obtained. Unlike the purely ambient noise cases, the dominant noise effects are signal-dependent here, which puts a premium on the choice of transmitted signal, S_{in}.

Before we proceed to results for the dominant scatter-channel (Section 3, et seq.), let us observe that the (linear) space-time filters (~ $g^{(Q)}$) presented formally so far can be replaced by purely (linear) temporal filter equivalents, under often reasonable conditions. This can be useful when we seek the medium's response, e.g., green's function, empirically, and attempt to model it analytically with simple functional forms, which may preserve the main effects of the medium and still yield manageable results for detector design and performance. In [1], Section 2.1, it is established that the necessary and sufficient condition's are:

A. *Ambient Sources:* The necessary and sufficient (n.+s.) conditions that that portion of the canonical channel (medium + coupling, cf. *Figure 2.1*) which contains ambient sources, local and distributed, be representable solely as a (realizable) temporal filter, is that these ambient sources be temporal only and independent of location, in the source domain Λ_A, e.g.,

$G_A(\mathbf{R},t) = G_{oA}(t)$, cf. Sec. 2**B**,[1] .

B. *Scatter Channels*: The (n.+ s.) condition for the canonical scatter, i.e, signal-dependent noise channels is, like the case of ambient sources, that the original, injected signals that excite the scattering elements be independent of location, cf. Section 2**C**,[1].

Specifically, for the ambient and scatter components of the canonical channel shown in *Figures 2.1* and *2.2*, which obey **A, B** above, the equivalences between the purely temporal and space-time filter weighting functions are:

A. *Ambient Sources* :
(Eq. (2.24),[1])

$$h_A(t-\tau,t) = \int_{V_R} d\mathbf{R} \int_{\Lambda_A} d\mathbf{R}' \int_{-\infty}^{\infty} h_{Rc}(t-\tau',t|\mathbf{R}) g^{(Q)}(\mathbf{R},\tau'|\mathbf{R}',\tau) d\tau' . \tag{2.7}$$

B. *Scatter Channels*:
(Eq. (2.31a),[1]

$$h_S(t-\tau,t) = \iint d\mathbf{R} d\mathbf{R}' \int_{-\infty}^{\infty} h_{Rc}(t-\tau',t|\mathbf{R}) g^{(Q)}(\mathbf{R},\tau'|\mathbf{R}',t') h_T(t'-\tau,\tau'|\mathbf{R}') d\tau' dt' . \tag{2.8}$$

Then, for the output of the receiving aperture or array $(\mathbf{T}_{AR})$, *Figures 2.1 and 2.2*, where now the canonical channel is described solely in terms of purely temporal filters (h_A, h_S, (2.7), (2.8)), we see that X(t) is given by the (temporal) convolutions.

$$\begin{aligned} X(t) &= h_S \circledast S_{in} + h_A \circledast G_{oA} \\ &= h_S \circledast S_{in} + h_d \circledast S_{in} + N_A(t) \end{aligned} \tag{2.9}$$

for the random and deterministic portions of the scatter channel. *Note that* $N_A(t)$ *can have a deterministic part* , e.g., $N_A(t) \neq 0$ in this model. Also, the ambient noise can, in part, be scattered by medium inhomogeneities, cf. (2.7). Physically, this corresponds to a coherent or specular component of the ambient sources, generated, say, by reflections off the ocean bottom and/or surface. The purely temporal equivalent of *Figure 2.2* is now

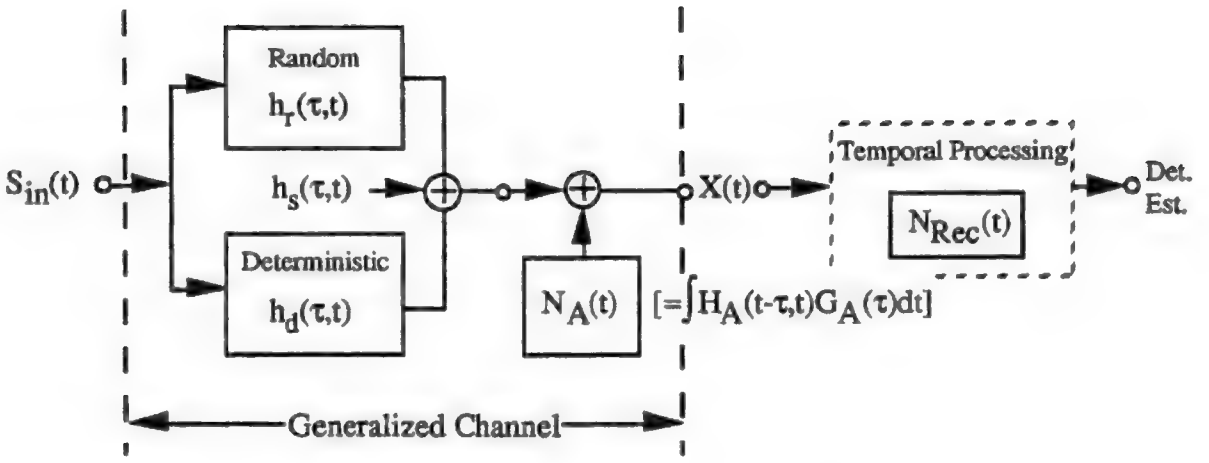

Figure 2.3 Purely temporal channel equivalent of the space-time generalized channel of *Figures 2.1* and *2.2*.

Special cases of (2.9) are familiar from telecommunications applications. We have

	gauss statistics: h_s or $g^{(Q)}$	non - gauss stastics: (h_s or $g^{(Q)}$)
I. $h_d = 0;=$	"Rayleigh fading" - troposcatter, ionospheric chanlels: unresolveable multipath (scatter); fading.	Nakagami models; same physical mechs.
II. $h_d \neq 0;=$	"Ricean fading" channel; VHF, UHF, HF groundwaves, etc; $h_d(\tau,t) = h_d(\tau)$.	Nakagami models; DM poisson models.
III. $h_r = 0;=$	time invariant channel, $h_s = \delta(\tau - t)$, plus $N_A(t)$ = AWGN (= add. white gauss noise); $h_s(\tau)$, purely frequency selective.	same N_A = "AWnonGN." same

(2.10)

A brief look at the implications of these results follows.

2.2 Implications:

A. The General Space-Time Formulation: $X = \hat{R}\alpha$, Eqs. (2.2)-(2.4), *Figures 2.1* and *2.2:*

The *advantages* of the general approach are:

1). Physical completeness; ∴ predictive, from propagation models;

2). Arrays - coupling to medium, array design, etc;

3). Spatial as well as temporal effects; explicit inclusion of $\nabla c \neq 0$, scattering etc.; and

4). Correct propagation of ambient sources in scattering medium.

The major *disadvantage* is the difficulty of obtaining $g^{(Q)}$ (or $\hat{M}^{(Q)}$, (3.2)) in the frequently encountered heavy scattering situations (e.g., multiple scattering), and the quantitative treatment of cases $\nabla c \neq 0$ involving a number of convergence zones. These limitations, however, are already overcome in many cases. See [1], [6], [8], in [1] here.

Further progress may be expected, computationally ([10], [11], in [1] here), as well as analytically.

B. The Purely Temporal Formulation: $X = h_S \circledast S_{in} + N_A$, (2.9):

The principal *advantages* of this more restricted channel model are:

1). Analytical and (comparative) statistical simplicity;

2). Ad hoc choices of h_S and the associated statistics justified by "local" experiments, i.e., measurements made at the receiver, for specific channels;

3). Direct ties-in to many of the channels and "target" modeling results of the 1960's and 1970's for radar, sonar, telecommunications, etc., Chapter 2, [4], Chapter 13, [5]. For example, a simple often-used model is the wide sense stationary uncorrelated scatter (WSSUS) channel, cf. Sec. 3 ff.

The main *disadvantages* are:

1). Tenuous relations, at best, to the underlying physical mechanisms: no insights as to what is happening;

2). Dependence on particular channel measurements -- non-predictive for others;

3). No explicit *spatial* structure: ∴ does not permit array design or, more broadly, (local) *matched field processing** (the spatial equivalent of "matched filtering" in time).

---

*This is *not* the same as "Matched Field Processing" (MFP), as used in passive source localization; see, for example, [18], [19] of [1].

3. SCATTER CHANNELS: A SUMMARY OF RESULTS [1], [2]

The received wave $X(t)$, after a signal $S_{in}(t)$ has been injected into the general channel, cf. *Figure 2.1*, has been represented by Eq. (2.9). The space-time equivalent can be expressed compactly in operator form by

$$X(t) = \hat{R}\hat{M}^{(Q)}G_T(-S_{in}) + \hat{R}\hat{M}^{(Q)}(-G_A), \tag{3.1}$$

where $\hat{M}^{(Q)}$ is the integral green's function associated with (2.4), viz,

$$\hat{M}^{(Q)}(\mathbf{R},t|\mathbf{R}',t') = -\iint dt'd\mathbf{R}'g^{(Q)}(\mathbf{R},t|\mathbf{R}',t')(\ )_{\mathbf{R}',t'}. \tag{3.2}$$

This operator is formally described by

$$\hat{M}^{(Q)} \equiv \left(\hat{1}-\hat{\eta}\right)^{-1}\hat{M}_{\infty}; \quad \hat{\eta} \equiv \hat{M}_{\infty}\hat{Q}, \tag{3.3}$$

where $\hat{M}_\infty$ is the integral green's operator of the associated homogeneous, i.e., infinite, medium, in which the inhomogeneity operator, $\hat{Q}$, vanishes, i.e., $g^{(Q)} \to g_\infty$ from (2.4) with $\hat{Q}=0$. Thus, $\hat{M}_\infty$ is defined by Eq. (3.2), with now $g^{(Q)} \to g_\infty$. These relations hold formally for random fields, as well, cf. remarks following Eq. (2.5b), where $g^{(Q)}$, $\hat{\eta}$, $\hat{M}^{(Q)}$ are stochastic functions and operators; $\hat{M}_\infty$ is deterministic. The full field, $\alpha(\mathbf{R},t)$, including both the "homogeneous" or unscattered part, α_H, and the "inhomogeneous" scattered component, $\alpha_I = \alpha - \alpha_H$, is formally obtained as the solution to Eq. (2.4), namely,

$$\alpha(\mathbf{R},t) = \left(\hat{1}-\hat{\eta}\right)^{-1}\alpha_H = \sum_{n=0}^{\infty}\hat{\eta}^{(n)}\alpha_H; \quad \alpha_H(\mathbf{R},t) = \hat{M}_\infty(-G_T). \tag{3.4}$$

Equation (3.4) is the Langevin (ensemble) equation for the random field α, and as explained above (Section 2), its "solutions" now are the various statistics of α, viz., $\langle\alpha\rangle$, $\langle\alpha^2\rangle$, $\langle\alpha,\alpha_2\rangle$, $w_1(g)$, etc. These are the quantities needed in determining effective models of the desired (target) signal and the accompanying reverberation and ambient noise, in order to approach optimal, or practical near-optimal, detection and classification, as noted in more detail in Section 5 ff.

3.1 SECOND MOMENTS AND WSSUS CHANNELS

Unfortunately, fully analytic solutions for $g^{(Q)}$, $\hat{M}^{(Q)}$, and therefore α and its statistics, are not generally achievable. We must accordingly seek compromise and approximate solutions. In the rest of this section, we summarize some of the principal results. We are concerned principally here with *narrowband* injected signals. For the details, see Section 3 of [1].

A statistic of major importance in describing the effects of our canonical channel on the injected signal, $S_{in}(t)$, is the *cospreading function* Ω_S, defined here by

$$\Omega_s(\tau_1,\tau_2;\,\nu_1,\nu_2) \equiv \langle H_s(\tau_1,\,\nu_1)H_s(\tau_2,\,\nu_2)^*\rangle \text{ , (Eq. (3.3c), [1]) ,} \tag{3.5}$$

where $H_s(\tau,\nu)$ is the well-known *spreading function* ([4], [5]), which measures how much the channel delay spreads in time ($\sim \tau$) and spreads in frequency ($\sim \nu$) whatever is transmitted through it.

When multiple scatter can be ignored, i.e., only single-scatter is the dominant component of the reverberation, then Eq. (3.4) becomes the (Born-) approximation

$$\alpha(\mathbf{R},t) \doteq \alpha_H + \hat{M}_-\hat{Q}\alpha_H \text{ , with } \alpha_I(\mathbf{R},t) \cong \hat{M}_-\hat{Q}\alpha_H \tag{3.6}$$

the reverberation contribution. Then it can be shown (Section 3.2, [1], and references) that the cospreading function Eq. (3.5) takes the form

$$\Omega_s(\tau_1,\tau_2;\,\nu_1,\nu_2) = \sigma_s(\tau_1,\nu_1)\delta(\tau_2-\tau_1)\delta(\nu_2-\nu_1) \text{ , } \sigma_s \geq 0 \text{ ,} \tag{3.7}$$

which is the result of independent scattering, namely, scattering with independent emissions, path delays, locations, and Dopplers. The quantity σ_s is usually called the *scattering function* and with (3.7) defines completely the second-order moment statistics of the channel (cf. refs. in [1]). Channels for which (3.7) holds are called *WSSUS* or *Wide Sense Stationary Uncorrelated Scatter* channels (cf. p. 18; [4]), and are often used to model EM telecommunication and underwater acoustic channels (for example, V, [2]; Sec. 2. [6]). Derivation of the scattering function is one major goal of scattering analysis, cf. *Sec. 3.2* following. However, WSSUS channels do not usually appear to be good models over long ranges in the ocean [7], and may not be for the shorter ranges considered here. The latter needs to be investigated, particularly when multiple scattering may be significant; see the remarks in Secs. 3.3, ff.

An important result in the WSSUS cases is the covariance of the received wave, $K_X(\tau_1,\tau_2) \equiv \langle X_1X_2\rangle - \langle X_1\rangle\langle X_2\rangle$, from which the intensity and power spectrum can be directly obtained. For narrowband signals, this WSSUS covariance and the associated scattering functions are related by (cf. Secs. 3.2-3.4,[1])

$$K_X^{(1)}(\tau_1,\tau_2) = E_X \mathrm{Re}\left\{ e^{i\omega_o(\tau_1-\tau_2)} \iint \hat{\sigma}_S(\tau,\nu)\left\langle s_o(t_1-\tau)_{in}\, s_o(t_2-\tau)^*_{in}\right\rangle_\phi e^{2\pi i\nu(\tau_2-\tau_1)} d\tau\, d\nu \right\} \tag{3.8}$$

$$\equiv E_X \mathrm{Re}\left\{ k_o^{(1)}(\tau_1,\tau_2)\exp\left(i\omega_o[\tau_2-\tau_1]\right)\right\} , \tag{3.8a}$$

where s_o is the complex envelope of the initially injected narrowband signal* (about the "carrier" f_o). Here $\tau \sim T_{oj}$, the path delay from source to scatterer to receiver, in the far-field, and E_X is the mean intensity of the array (or aperture) output, X(t) , related to σ_s by $\hat{\sigma}_s = \sigma_s / E_X$, where

---

* "Narrowband " is defined here as a ratio of central frequency f_o to bandwidth Δf , which obeys $f_o/\Delta f \gtrsim 4$, approximately.

$$E_X \equiv \iint \sigma_s(\tau,\nu)\left|s_o(t_1-\tau)_{in}\right|^2 d\tau\, d\nu\,. \tag{3.8b}$$

The average $\langle\ \rangle_\phi$ is an ensemble average over the phase or epochs of the injected signal envelopes (see Eqs. 3.10 and 3.11 ff). In terms of the *ambiguity function*, defined here by

$$\chi_o(\tau,\nu) \equiv \int_{-\infty}^{\infty} s_o(t'-\tau)_{in}\, s_o(t')^*_{in}\, e^{2\pi i\nu t'} dt' = \int_{-\infty}^{\infty} s_o(f)_{in}\, s_o(f+\nu)^*_{in}\, e^{-i\omega\tau} df\,,\ \omega = 2\pi f\,, \tag{3.9}$$

where $\chi_o(0,0) = \int_{-\infty}^{\infty}\left|s_o(t')_{in}\right|^2 dt' = 1$ is the intensity of the normalized envelope amplitude s_o, we can express the WSSUS covariance (3.8) as

$$K_X^{(1)}(t_1,t_2) = E_X \int S_\delta(-\nu, t_2-t_1)\overline{\chi_o(t_2-t_1,\nu)}^{\phi} e^{-2\pi i\nu t_2} d\nu \tag{3.10}$$

Here

$$S_\delta(f,t) \equiv \mathcal{F}_\nu^{-1}\mathcal{F}_\tau\left\{\hat{\sigma}_s(\tau,\nu)\right\} = \iint \hat{\sigma}_s(\tau,\nu) e^{-i\omega\tau+2\pi i\nu t} d\tau\, d\nu \tag{3.10a}$$

is the double Fourier transform $(\mathcal{F})$ of $\hat{\sigma}_s$, as indicated.

3.2 FULL CHANNEL COVARIANCE: NARROWBAND SIGNALS

One of our main tasks in channel modeling is to determine not only the WSSUS covariance (Eqs. (3.8) and (3.10)), but the complete covariance, including the contributions of multiple scatter. This can be noticeably advanced with the help of a suitable *counting functional*, which allows us to specify the (formal) interactions of individual scattering elements with one another and the incident radiation. The detailed development is provided in Secs. 3.2 and 3.3 of [1]. The complete covariance is found to be (cf. (3.30),[1]) for these narrowband injected signals

$$K_X(t_1,t_2) = \frac{1}{2}\mathrm{Re}\left\{\begin{array}{l} e^{i\omega_o(t_1-t_2)}\iint \hat{\sigma}_S(\tau_1,\nu_1) e^{2\pi i\nu_1(t_2-t_1)}\left\langle s_o(t_1-\tau_1)_{in}\, s_o(t_2-\tau_2)^*_{in}\right\rangle_\phi d\tau_1\, d\nu_1 \\ +e^{i\omega_o(t_1-t_2)}\int\!\cdots\!\int \Omega_S^{(\infty)}(\tau_1,\tau_2;\nu_1,\nu_2) e^{i\omega_o(\tau_1-\tau_2)+2\pi i(\nu_2 t_2-\nu_1 t_1)} \\ \qquad \bullet\left[\left\langle s_o(t_1-\tau_1)_{in}\, s_o(t_2-\tau_2)^*_{in}\right\rangle_\phi d\tau_1\ldots d\nu_2\right]. \end{array}\right. \tag{3.11}$$

The first term embodies the WSSUS or single-scatter component, while the second represents all the multiple-scatter contributions $(k \geq 2)$, viz. $\Omega_S^{(\infty)} \equiv \sum_{k=2}^{\infty} \Omega_S^k$, where $\Omega_S^{(\infty)}$ is now the cospreading function, cf. (3.5), for the latter interactions.

Using our earlier results, cf. Eq. (4.47) of [8], for narrowband (n.b.) signals in the far-field (f.f.), we have for a typical bistatic received waveform from the j^{th} point scattering element here

$$U_j\Big|_{\substack{n.b.\\f.f.}} \doteq \frac{\mu\gamma(\lambda)e^{i\phi_o}}{(4\pi)^2 R_T R_R}\exp[i\omega_o(1-\varepsilon)(t-T_o(\lambda))]\mathcal{A}_T\mathcal{A}_R\Big|_{f_o} s_o(t-T_o(\lambda))_{in}\ , \qquad (3.12)$$

where $\varepsilon = (\sim v_d / c_o)$ is a random Doppler; $\mu = 1-\varepsilon$; $\gamma_o(\lambda)$ = "cross-section" of the scatterer, and $\mathcal{A}_T, \mathcal{A}_R$ are the (complex) beam patterns (cf. *Figure 2.1*) of transmitter and receiver, e.g., $\mathcal{A}_T = \mathcal{A}_T(v_T - v_{oT}|f_o)$, with $v_T = \hat{i}_T f_o / c_o$, and v_{oT} is a steering wave number, etc. For details of the geometry, see *Figure 1* of [2]. Here λ is a distance $(= |\mathbf{R}| / c_o)$ measured in units of time. Thus, $T_o(\lambda) = (|\mathbf{R}_T| + |\mathbf{R}_R|) / c_o$. For use in the time-frequency forms above, Eq. (3.5) et seq., we can replace T_o by τ , ω_o by $2\pi\nu$, etc. (cf. comments following Eq. (3.28), [1]). From Eq. (3.12), then, it is readily shown that for the WSSUS component, the scattering function σ_s now becomes explicitly

$$\sigma_s(\tau,\nu) = \frac{A_2^{(1)}\left(1-\frac{2\pi\nu}{\omega_o}\right)\overline{\gamma^{(1)2}}\left(|\mathcal{A}_T\mathcal{A}_R|^2\right)_{\tau,\nu} G(\tau)}{(4\pi)^4 R_T(\tau)^2 R_R(\tau)^2} \geq 0\ ,\ k=1\ , \qquad (3.13)$$

with $G(\tau)$ the contribution of the Jacobian $|J|$ from rectangular to spherical coördinates [8], and the conversion of $\lambda = \lambda(\tau)$, $d\lambda = d\tau / f'(\tau)$, etc., all of which depend, of course, on the geometry of source, receiver, and the illuminated scatterers on the boundaries and in the volume [6],[8].

Various useful generalization and special results, which are beyond the scope of the present summary, as well as extensions of the methods employed to derive Eqs. (3.8) and (3.11) above, are presented in detail in Section 3.3 and Section 4 of [1].

3.3 SUMMARY OF PRINCIPAL RESULTS FOR CHANNEL MODELING: SECS. 2, 3, AND SECS. 2-4 OF [1]

To operate effectively in a physical channel environment (= medium plus coupling), we must estimate the pertinent features of the channel. Thus, our ultimate signal processing is necessarily *adaptive*. Accordingly, probing or "remote sensing" of the channel's response (h_s) is suggested. As long as the channel is stable during intervals of use, we may expect good results. Over time, we require updating of channel parameters, which is usually done on a continuous averaging basis. Without adaptivity, we cannot make full use of our processing capabilities. We may then expect serious degradation of performance vis-à-vis the adaptive cases, which in the broad sense are "matched" to actual channel characteristics. In the above when purely temporal specification of the channel is employed, through the channel's response function $h_s(t,\tau)$, we have, in effect, preformed beams: the array or aperture has a postulated structure, so that only

"matched filtering," i.e., temporal matching for optimization, is possible. On the other hand, if the coupling structure is left adjustable to the incoming signal and noise fields, then spatial matched filtering, or (local) "matched field" processing* is possible as well. For this, of course, we need pertinent statistics of the noise (and signal) fields, such as their covariance functions.

It is with this background that we summarize our principal results above on channel modeling, which may serve as a guide to both modeling and measurement, for ultimate application in the required signal processing. We note the following :

I. For there to be a *purely temporal representation of the channel* equivalent to the fundamental space-time representation, the driving sources (ambient and active) must be independent of location. This is both necessary and sufficient, cf. Sec. 2.1, **A**, **B**.

II. *The temporal channel equivalent* $(h_s(t,\tau))$ *is "global"*--contains all spatial effects--while the green's function, $g^{(Q)}$, Eqs.(2.4),(2.6) of the medium itself is "local," i.e., at a point $P(\mathbf{R},t)$, although its value at a point includes the effects, at that point, of all scatter interactions elsewhere as well.

III. *Scattering media* (including boundaries) *are nonreciprocal*: source and receiver are not interchangeable, and no generalized Huyghens principal (GHP) exists for the solution of the field propagation equations in such media. Alternative (operational) methods must be employed [9], cf. Eq. (3.6) of [1].

IV. *Single-scatter channels are always WSSUS* (in the steady state). They accordingly have a *cospreading function* $\Omega_s^{(1)}$,which obeys Eq. (3.7) and defines a scattering *function* $\sigma_s(\tau,\nu)$; (see Refs. [10] and [11] for such a surface scatter mechanism generated by wind).

V. *WSSUS channels may not be satisfactory models for long-range* (to CVZ and beyond) *underwater acoustic propagation*, because of coupling (multiple-scatter effects, which are path-dependent.

VI. Accordingly, *the WSSUS character of the channel should be empirically tested*--as part of the adaptive, remote sensing for channel matching; (see Refs. [10] and [11] for surface scatter).

VII. The scattering function $\sigma_s(\tau,\nu)$ can be calculated, as well as measured; (see Sec. 3.2 above).

---

* See footnote, p. 7, for comments.

VIII. The general second-order (output) covariance $K_X(t_1, t_2)$ is explicitly obtained (Sec. 3.2) when there is a non-WSSUS, as well as WSSUS, component.

IX. Generalizations of VIII are derived in Sec. 3.3 of [1].

X. Extensions and equivalences with counting functional results are derived in Sec. 4 [1].

Finally, the above suggests some further topics for study along these lines:

1. Extension of WSSUS concepts to include spatial variations: (local) "matched field" concepts.
2. Extension of the global channel representation $(\sim h_s)$ to specific evaluation of media: media "probes."
3. Further direct calculation of specific classes of scattering function σ_s , and cospreading functions (based on [2], [6], and [8]), as well as on the approach outlined in detail in Sec. 3.2, [1].

4. ELEMENTARY TARGET MODELS: TARGET STRUCTURE FACTORS (SECS. 6,7 OF [1])

The aim is to construct simple but "realistic target models, which exhibit reflection and scattering. These models are "quasi-phenomenological" in some details, directly physical in others. The basic idea is to preserve the relevant target features, e.g., "cross-section," spatial distribution, motion, which are dominant, as is the central rôle played by the associated geometry. Much of the so-called "fire-structure" is smoothed out by the inevitable uncertainty in parameter values, through statistical averaging. This is not a new problem, nor are our results here particularly innovative: the comparatively naïve model employed here consists of a linear distribution of reflecting "sources," with adjustable parameters of scale and function.

Our particular goal is to obtain analytic expressions for the received narrowband (i.e., complex) envelope $(s_o =)s_o(t)_L$, Eq. (3.8) et seq., of a linear target, arbitrarily oriented with respect to the transmitter and receiver, in the manner of *Figures 4.1* and *4.2*.

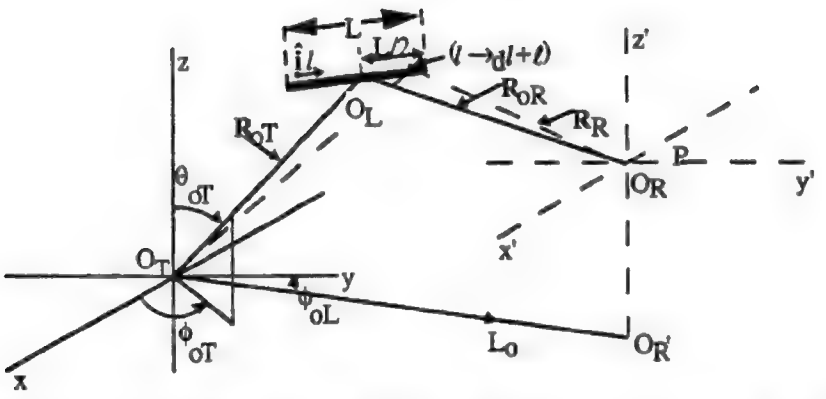

Figure 4.1 Sketch of a bistatic transmitter (T), target (L), and a receiver (R) geometry. (This is *Figure 1* of [6], with the surface area replaced by a line, L.)

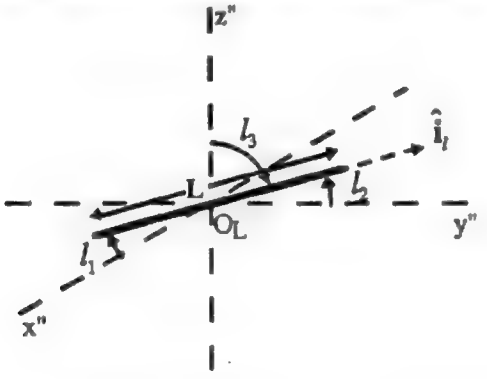

Figure 4.2 Target orientation vis-à-vis $O_L \to O_T, O_R$.

The result (cf. Eq. (6.19) of [1]) is the *continuous linear model*, for which

$$\boxed{\begin{aligned} s_o \to s_o(t-T_o;\varepsilon)_L \doteq \exp\{i\omega_o(T_o-\varepsilon)\}\sqrt{G^{(1)}(f_o)}\int_L \mathcal{A}_{RT}(\ell)e_{d\ell}^{-2ik_o\alpha_o\bullet\ell} \\ \cdot\int_{-\infty}^{\infty} e^{-ik_o(2\alpha_o\bullet v_d)(t-T_o-\tau)} h_o(\ell,t-T_o-\tau)_L s_o(t-\varepsilon)_{in}\,d\tau \end{aligned}} \tag{4.1}$$

is the complex signal envelope of the target as seen at the receiver. Here $\mathcal{A}_{RT} = \mathcal{A}_R\mathcal{A}_T$, while

$$G^{(1)}(f_o) \equiv \frac{\exp(-2a\omega_o^2 c_o T_o)}{(4\pi)^4 R_{oT}^2 R_{oR}^2}\ , \text{ Eq. (29b),[6], } \omega_o = 2\pi f_o\ , \tag{4.1a}$$

and $\ell = \hat{\mathbf{i}}_\ell \ell = \hat{\mathbf{i}}_x \ell_x \ell_1 + \hat{\mathbf{i}}_y \ell_x \ell_2 + \hat{\mathbf{i}}_z \ell_z \ell_3$, with $\ell_{1,2,3}$ the direction cosines of ℓ vis-à-vis (x,y,z) of O_T. The quantity $\hat{t}$ in Eq. (4.1) represents different possible Doppler effects, specified by Eq. (6.10) of [1]. Other quantities in Eq. (4.1) are given by Eq. (4.5) ff:

$$2\alpha_o = \left(\hat{\mathbf{i}}_{oT} - \hat{\mathbf{i}}_{oR}\right); \tag{4.2a}$$

v_D = doppler velocities: for no platform motion,

$$v_D t \to (t - R_{oR}/c_o)v_d \; ; \quad \text{but see Eq. (67.10b),[1]} \; ; \tag{4.2b}$$

$T_o = (R_{oT} - R_{oR})/c_o$

$$= \text{(mean) wavefront path time: } O_T \to O_L \to O_R \; ; \tag{4.2c}$$

c_o = speed of sound in (isovelocity medium ($\nabla c = 0$)) ; (4.2d)

$s = 2\pi i f \; ; \; s_o = 2\pi i f_o \; ;$

f_o = *central frequency of injected (n.b.) signal*; (4.2e)

a = absorption coefficient; (4.2f)

ν_{oT}, ν_{oR} = (wave no.) beam steering ; (4.2g)

$\mathcal{A}_T, \mathcal{A}_R$ = (*preformed*) beam patterns (which are complex) ; (4.2h)

(See also Appendix I, [6], for definitions and relations),

$$\text{e.g., } t' = t - \Delta t_{dS}, \text{ cf. (3.14), [6]} \; . \tag{4.2i}$$

The quantity h_o is the (real) narrowband portion of the (real) *target's scatter kernel*

$$q_L(\tau, t) = q_L(t - \tau) = 2h_o(t - \tau)_L \mathrm{Re}\left\{\exp\left[i\omega_o(t - \tau) - i\gamma_o(t - \tau)\right]\right\} \; , \tag{4.3}$$

cf Eqs. (6.9), (6.18) of [1].

An alternative to the continuous aperture or scatter kernel q_L (4.3) is the *discrete model*, where now the aperture takes the form

$$q_L(\tau, t) = q_L(t - \tau) = \sum_{k=1}^{K} a_k e^{i\phi_k} \delta(\ell - \hat{i}_\ell k\Delta\ell)\delta(t - \tau - T_o) \; , \tag{4.4}$$

with $\hat{i}_\ell$ = unit vector along ℓ as before, cf. (4.1) et.seq., and *Figure 4.2*, e.g., $\ell = \hat{i}_\ell \ell$ above. The discrete equivalent of (4.1) is then found to be (cf. sec. 7, [1])

$$\boxed{\begin{aligned} s_o(t - T_o \; ; \; \varepsilon)_L \doteq \sqrt{G^1} e^{-i\omega_o \varepsilon} \sum_{k=1}^{K} a_k e^{i\phi_k} \mathcal{A}_{RT}(k\Delta\ell) e^{-2i\alpha_o \cdot \hat{i}_\ell k\Delta\ell} \\ \cdot \exp\left[ik_o\left(2\alpha_o \cdot \hat{i}_\ell\right) v_d R_{oR}/c_o\right] s_o(t - T_o - \varepsilon)_{in} \; , \end{aligned}} \tag{4.5}$$

since $\underset{\sim}{v}_d = \hat{i} v_d$. In the far-field, $\mathcal{A}_{RT}(k\Delta\ell) \to \mathcal{A}_{RT}^{(o)}$, a constant (dependent on the "carrier" or central frequency, f_o and target length L). Here the weights $a_k = (\bar{a}_k + \Delta a_k)$ may be regarded as mixed deterministic and random, at positions $\ell = k\Delta\ell$, k = 1 , ... , K along L . For example, the Δa_k may be regarded as independent gaussian quantities, or the a_k , each k , may be regarded as obeying Poisson statistics

bf 3/21/92

$$w_1(a_k) = \frac{(\nu_k \Delta\ell)^m}{m!} e^{-\nu_k \Delta\ell} , \Delta\ell \nu_k = \bar{a}_k , \text{ etc.,} \tag{4.6a}$$

with

$$\phi_k : w_1(\phi_k) , 0 \le \phi_k \le 2\pi , \tag{4.6b}$$

to be selected, appropriate to the model chosen.

The quantity $F_\sigma(t)$ is called the *Target Structure Factor (TSF)* and is defined by the ratio

$$F_\sigma \equiv \left|\overline{s_{o\text{-}L}}\right|^2 \Big/ \left|\overline{s_{o\text{-}in}}\right|^2 \tag{4.7}$$

for these coherent reception modes, with $s_{o\text{-}L}$ given specifically by Eqs. (4.1) or (4.5) here. As we shall see presently (Secs. 5.2.A,B, F_σ plays a central rôle in effective detection in a reverberation dominated scenario.

Various extensions of the models (4.1), (4.5) need to be considered. Not necessarily in order of importance, among these are:

1. Moving target *and* platform scenarios ;
2. Deterministic and random dopplers ;
3. Explicit statistical models of scattering strengths : h_o , (4.1), a_k ,(4.4);
4. Intensities and covariances of these generic target models for incoherent detection ;
5. Continuous models $(\sim h_{o\text{-}L}$, (4.1)) , (4.3) continuous in $\ell (\in \mathbf{L})$;
6. More detailed physics of q_L , (4.3): "highlights," wakes, resonances etc. ; and
7. Kirchoff boundary conditions on ℓ .

(4.8)

For a more complete account of these models and derivations, see Secs. 6 and 7 of [1].)

5. TARGET DETECTION: THRESHOLD ALGORITHMS AND PERFORMANCE MEASURES

Our aim in this section is to provide a concise summary of analytical results for optimal and near-optimal detection of target signals in noise and interference. Specifically, we are concerned with the combination of ambient (gauss and nongaussian) background noise and signal-dependent noise, or reverberation, when the latter is strong vis-à-vis the desired target signal. The principal noise or interference here is canonically nongaussian, in the sense of the author's familiar Class A

5.1 THRESHOLD DETECTION IN SIGNAL-DEPENDENT NOISE

We begin with a short summary of the detection situation in signal-dependent noise, represented by the usual binary "on-off" hypothesis models here. These are

I. *General On-Off Detection: Signal-Dependent Noise*:

This is expressed by:

H_o: (no signal): $N(S) + N_A + N_R$ vs. H_1: (signal + noise): $N(S) + N_A + N_R + S$.

reverb. ambient noise receiver (5.1)

II. *Strong Scatter: Approximate Decision Situation*:

$$\boxed{H_o: N(S) + N_{A+G} \text{ vs. } H_1: N(S) + N_{A+G} + S\,,} \tag{5.1a}$$

where $N_{A+G} = N_A + N_G$ is a mixture of gauss (N_G) and nongaussian noise in the usual way, with a usually dominant nongaussian component. The reverberation [N(S)] is either gaussian or nongaussian, depending on geometry and ("carrier") frequency of these n.b. signals [15].

In general, the *intensity* of the accompanying noise can be represented here by

$$\Psi = \Psi(S) + \Psi_{A+G} = \overline{N(S)^2} + \overline{N^2_{A+G}}\,. \tag{5.2}$$

where

$$\Psi(S) = \overline{N(S)^2} = (F_S + F_V + F_B)\overline{\tilde{A}_o^2},\ F \geq 0\,. \tag{5.2a}$$

Here F_S, F_V, F_B are respectively the "structure factors" of the acoustic reverberation off the ocean wave surface, the volume, and the bottom. At least two of these terms (including F_V) will be present, again depending on the geometry of source (cf. *Figure 5.1*, the possible target, and the dispersive character of the medium. For many of our applications the surface component dominates, so that $\Psi(S) = \overline{\tilde{A}_o^2}\, F_S + \Psi_{A+G}$ .The detailed nature of these structure factors is determined, likewise, by geometry, source frequency, and waveform, and the appropriate scatter model which governs these reverberation terms; see Section 5.3 ff. and references.

Figure 5.1 shows some typical propagation geometries, where $\nabla c \neq 0$; (here $c = c_o + \nabla c(R)$, is the speed of wavefront propagation). Depending on target location, the various components of reverberation may be expected to occur. We remark that bottom reverberation is almost always nongaussian, while surface and volume reverberation can be gaussian, if the effective number of ensonified scatterers is sufficiently large and no few scatterers predominate over the others. At high frequencies and small angles (primarily for surface and bottom scatter), however, we may frequently expect a small number of large scattering elements ("facets") to dominate in the beam, so that an often strongly nongaussian reverberation results.

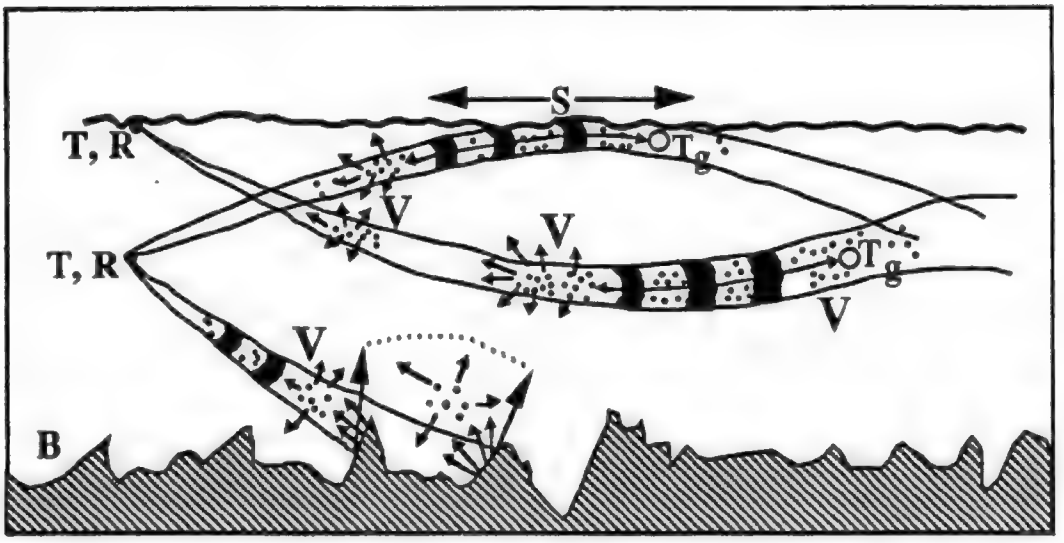

Figure 5.1 Sketch of some typical ("high-frequency" or n. b.) propagation of beamed signals, when $\nabla c \neq 0$, showing potential mechanisms of reverberation: T, R = transmitter, receiver; Tg = target.

A. On-Off Binary Detection Algorithm; Coherent Threshold Detection - Canonical Forms:

From earlier work [2] the canonical form of the optimum "on-off" threshold detection algorithm is well-known to be [2], [14].

$$\log \Lambda_J(\mathbf{x}|\theta) \doteq g_J^*(\mathbf{x})_{coh} = \hat{B}_{J-coh}^{(*)} + \log \mu - \sum_{m,n=1}^{M,N} l\left(x_{m,n}\right)\left\langle \theta_{m,n} \right\rangle , \tag{5.3}$$

$$\begin{cases} \hat{B}_{J-coh}^{(*)} \triangleq -\dfrac{1}{2}\hat{\sigma}_{J-coh}^{(*)2}: \text{ bias term; (space) } m = 1,\ldots,M; \text{ (time) } n = 1,\ldots,N; \ \mu = p/q; & (5.4a) \\ \hat{\sigma}_{J-coh}^{(*)2} \equiv \mathrm{var}_{H_0} g_{J-coh}^{(*)} = 2L(*)J\left\{\dfrac{1}{J}\displaystyle\sum_{m,n}^{J}\left\langle a_{on}^{(m)}\right\rangle^2\left\langle s_n^m\right\rangle^2\right\}, \qquad (J = MN) & (5.4b) \end{cases}$$

$$\begin{array}{ccc} \downarrow & \downarrow & \\ 2\Pi_{J-coh}^{*} & \left\langle a_0^2 \right\rangle_{min-coh}^{*} & (5.4c) \\ \downarrow & \downarrow & \\ \text{"processing gain"} & \text{"min. detectable signal (power)"} & \end{array}$$

$$l\left(x_{m,n}\right) \equiv \frac{d}{dx}\log w_1(x|H_0)\Big|_{x=x_{m,n}} ; \ L^{(2)} \equiv \left\langle l^2 \right\rangle_{H_0} = \int_{-\infty}^{\infty} \ell(x) w_1(x|H_0)dx ; \tag{5.4d}$$

$$\langle \theta_{m,n} \rangle = \langle a_o^{(m)} \rangle (t_n) \langle s^{(m)}(t_n) \rangle_e \text{ , with } \langle s_n^{(m)2} \rangle = 1 \text{ ,}$$

(cf. remarks ff. Eq. (60d), [2],), (5.4e)

with

$$a_o^{(m)}(t_n) \equiv a_{on}^{(m)} \equiv \frac{A_o^{(m)}(t_n)}{\sqrt{2\Psi}} = \frac{A_{on}^{(m)}}{\sqrt{2\Psi}}, \text{ cf. (5.12b)ff} \quad (5.4f)$$

in which, as before [2], [13], m denotes the m^{th} sensor or "space-sample," while n represents t_n ($=n\Delta t$), the n^{th} "time-sample," in the space-time observation interval. Here we have

$$\mathbf{x} = \mathbf{X}/\sqrt{2\Psi} = \{x_{m,n}\} = \{x_j\} \text{ , with } \Psi = \text{Eq. (5.2); } j = m,n, \text{ etc.,} \quad (5.5)$$

where $\mathbf{x}$ is the normalized, sampled, input field data. Also, μ ($=p/q$) is the ratio of *a priori* probabilities that the input does or does not contain a desired signal (target). Finally, $w_1(x|H_0)$ is the (first-order) pdf of x, the typical noise data sample, which usually consists of an additive mixture of nongauss (reverberation and ambient) noise and a normal component.

Figure 5.2 shows the flow diagram of the optimum threshold algorithm g_J^*, here for coherent detection in generalized, e.g., signal-dependent, nongaussian noise. As usual, coherent detection requires that the signal epoch $\varepsilon = \varepsilon_O$, a known quantity at the receiver, adjusted to maximize the carrier waveform, [13], [14], [4]. The various components of g_J^* represent the following signal processing operations:

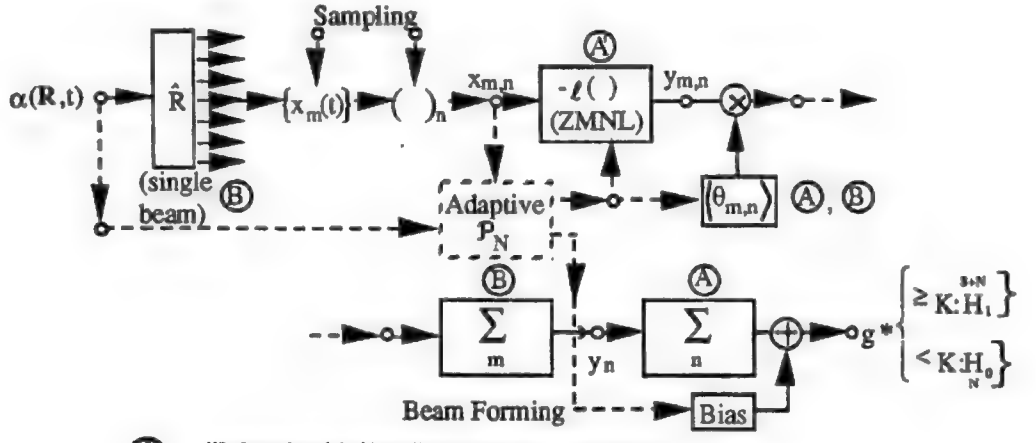

Figure 5.2 Flow diagram of the canonically optimum, coherent threshold detection algorithms, with adaptive beam forming (m), generalized, signal-dependent noise.

Eq. (5.6):

(1) $\hat{\mathbf{R}}$ = array operator: samples the input acoustic field $\alpha(\mathbf{R},t)$, at points $\mathbf{R} \rightarrow \{r_m\}$, m=1,...,M; see Part II, Section 3.1 of [1].

(2) $(\ )_n$ = time sampling: the result is a (normalized) space-time sampled waveform sample, which then undergoes the signal processing described below:

(3) $-l_{(ZMNL)}$ = "matching-to-the-noise," via $l(x)$, Eq. (5.4d), to yield $y_{j=m,n}$; cf. Ⓐ in *Figure 5.2*.

(4) $\otimes\langle\theta_{m,n}\rangle$ = cross-correlation with appropriate model of the received signal, i.e., one that includes such effects as possible "Doppler smear," "fading" or unresolvable multipath, and beam steering, etc., cf. Sec. 5.2A, embodied in the Target Structure Factor (TSF), cf. (5.11), (5.7).

(5) Σ_m = "beam forming," when combined with appropriate path delays ($\sim r_m/c_o$) in $\hat{\mathbf{R}}$ (2.2) to produce a temporal wave, y_n. In conjunction with $\hat{\mathbf{R}}$ and proper delays (in $<\theta_{m,n}>$), cf. Ⓑ in *Figure 5.2*, this represents *adaptive beam-forming*.

(6) Σ_n = in conjunction with (4) constitutes "matched-filtering," or "matching-to-the signal," cf. Ⓐ in *Figure 5.2*.

(7) ⊕Bias = addition of a suitable bias, $\hat{B}_J^*$, to ensure both optimality and consistency of the test H_1 vs. H_0 .

(8) g_J^* = a number, produced by the operations (1) - (7), which is then compared to a threshold K which is preselected to yield a predetermined false alarm probability, α_{F^*}, cf. Sec. 5.2 ff. The resulting decision is H_0: $g^* < K$ or H_1: $g \geq K$, etc.

We remark that the system produces decisions continuously as the input data stream is continuously updated, for the given (moving) period $(t_o, t_o + T)$; or one can operate it in a series of decisions at intervals T, etc.

More important is the critical feature of all these optimum (and similarly related suboptimum) systems, namely, that they are *adaptive*: they require the measurement and updating of the relevant signal and noise parameters. These are, for example, noise level, Ψ, received signal level ($\sim A_O$), the (nongaussian) noise parameters, $\mathcal{P}_{A,B}$, associated with the governing class of noise, expressed in terms of $w_1(x|H_0)$ here, cf. [14], whether it be Class A or Class B -- probably Class A, for a dominating reverberation. (For details see [14]; also, Part II of [2] and refs.) In essence, the effectiveness of these coherent (and incoherent) detection algorithms depends on how

well we can estimate the relevant parameters of the "environment" so that good adaptation is achieved. Provided the time-scale of change of the environmental parameters is slow (i.e., "isothermal rates") vis-à-vis the observation period needed to achieve effective levels of correct signal detection probabilities -- which is fortunately the case, most of the time -- our threshold systems here can practically approach optimality quite closely [13].

Finally, we note that those optimum threshold systems no longer remain optimal for stronger (to strong) signals. However, on an absolute basis they are quite satisfactory, as long as care is taken to avoid possible destruction of the information in the desired signal, which can occur because of the saturating nature of the (ZMNL) $l(x)$. In general, larger detection probabilities result for increased signal strength under these conditions.

5.2 Performance Measures

In order to predict the effectiveness of our detection algorithms, (5.3) et seq. and *Figure 5.2*, we need suitable performance measures. These are, comprehensively for most purposes, the probability of correctly detecting the presence of the (target) signal (S). For these threshold cases (which likewise provide algorithms for the stronger signals, cf. end of Sec. 5.1 above), it is found that ([2], Part 2, Sec. VIII) this detection probability is specifically

$$P_D \equiv \frac{p}{2}\left\{1+\Theta\left[\frac{\sigma_J^{(*)}}{\sqrt{2}}-\Theta^{-1}\left(1-2\alpha_F^{(*)(*)}_F\right)\right]\right\}, \text{ (Eq. (69), [2] ,} \tag{5.7}$$

with the associated (conditional) false alarm probability

$$\alpha_F^* \equiv \frac{1}{2}\left\{1-\Theta\left[\frac{\sigma_J^{(*)}}{2\sqrt{2}}+\frac{\log\left(K/\mu\right)}{\sqrt{2}\sigma_J^{(*)}}\right]\right\}, \mu = p/q; \text{ (Eq. (71), [2] .} \tag{5.8}$$

Here $\sigma_J^{(*)}$ is the *detection parameter* governing performance, given by

$$\sigma_J^{(*)} = \mathrm{var}_{H_0}\, g_J^* = -2\hat{B}_J^{(*)}\Big| \text{ , cf. (5.4a) and (5.4b) in the coherent cases) .} \tag{5.9}$$

The quantities K and μ (=p/q) are respectively the threshold, which establishes the desired false alarm probability $\alpha_F^{(*)}$, and the *a priori* data probability ratio μ [14].

A. Structure of the Detection Parameter, $\sigma_J^{(*)2}$:

It is the detection parameter we wish to maximize, or at least make as large as practically possible, by choosing suitable input signal waveforms so that the combination of "output" (i.e., received) signal structures vis-à-vis the now dominating signal-dependent noise ($\Psi(S)$, (5.2))

produced by reverberation, cf. *Figure 5.1*, according to the governing geometry of propagation, is made as large as possible. For the coherent régimes considered here, (5.4b) is the governing form of the detection parameter, generally, viz.:

$$\sigma^{(*)^2}_{J\text{-}coh} = 2L^{(2)}J\left\{\frac{1}{J}\sum_{m,n}\left\langle a_o^{(m)}\right\rangle^2\left\langle s_n^{(m)}\right\rangle^2\right\}, \tag{5.10}$$

where $s_n^{(m)}$ is the real normalized [cf. (5.4a)] signal received at the m^{th} sensor, at time t_n, while $a_{on}^{(m)}$ is the associated (normalized) amplitude, cf. (5.4f).

Our task now is to relate the real received signal $s_n^{(m)}$ to the complex injected signal $\left(\hat{S}_{o\text{-}in}\right)$, in order to establish canonically the rôle of the target in modifying the originally transmitted signal, cf. *Figure 5.1*. The explicit result depends, of course, on the target model chosen as well as on the propagation conditions. From Section 4, we have the desired target structure factor (TSF), (4.7), (5.4f), etc. as the ratio of two square-of-the-mean signal envelopes in these coherent detection cases:

$$\left.\begin{aligned} TSF:\ F_\sigma^{(m)}\left(\hat{t}_{m,n},\hat{t}_n\right) &\equiv \left|s_o^{(m)}\left(\hat{t}_{m,n}\right)_L\right|^2 \Big/ \left|s_o^{(m)}\left(\hat{t}_n\right)_{in}\right|^2 \ ;\ \ \hat{t}_{m,n} = t_n - T_o - \varepsilon + \Delta\tau_m \\ &\equiv F_\sigma^{(m)}\left(t_{m,n}\right);\ \ \hat{t}_n = t_n - T_o - \varepsilon\ ;\ T_o = \left|\mathbf{R}_{oT}\right|/c_o + \left|\mathbf{R}_{oR}\right|/c_o\ . \end{aligned}\right\} \tag{5.11}$$

Here T_o is the path delay between source and receiving array $\left(O_T \to O_R\right)$, and the delays $\Delta\tau_m$ are specifically given by

$$\Delta\tau_m = \left(\hat{\mathbf{i}}_o - \hat{\mathbf{i}}_{oR}\right)\cdot \mathbf{r}_m/c_o\ , \tag{5.11a}$$

where $\hat{\mathbf{i}}_o$, $\hat{\mathbf{i}}_{oR}$ are respectively the wavefront normals of the received signal and beam direction (of the maximum lobe of the adaptively formed beam here), [13]. The result for $s_n^{(m)}$, the (real) normalized signal at the m^{th} sensor at time t_n, is found to be (Sec. 9.1, [1])

$$\boxed{s_n^{(m)} = \mathrm{Re}\left\{\sqrt{2}s_o\left(t_n - T_o - \varepsilon_o\right)_{in}\exp\left\{i\omega_o\left(t_n - T_o - \varepsilon_o\right)\right\}\right\} = s_{on}\ ;} \tag{5.12}$$

$$\boxed{\frac{\overline{A_{on}^{(m)^2}}}{2\Psi} = \frac{\overline{\tilde{A}_o}^2 F_{\sigma\text{-}n}^{(m)}}{2\Psi}:\qquad \therefore A_{on}^{(m)} = \tilde{A}_o\sqrt{F_{\sigma\text{-}n}^{(m)}}\ .} \tag{5.12a}$$

In this way we have identified the various components of the normalized *received* signal with the original transmitted signal, so that, with $\Psi = \Psi_{A+G} + \Psi(S)$ of (5.2) and (5.2a) above, we see that the detection parameter (5.10) now becomes explicitly (albeit still in canonical form)

$$\sigma^{(*)2}_{J\text{-coh}}\Big|_{\substack{\text{(adaptive}\\ \text{beam}\\ \text{forming)}}} = 2L^{(2)}MN\left\{\frac{(1-\eta_o)}{\left\{F_S+F_V+F_B+\Psi_{A+G}/\bar{\tilde{A}}_o^2\right\}}\sum_{m,n}^{M,N}\frac{\overline{\left|s_o(t_n-T_o-\varepsilon_o)_{in}\right|^2}\,F_\sigma^{(m)}(t_n-T_o-\varepsilon_o;\Delta\tau_m)}{2MN}\right\} \tag{5.13}$$

$$\left((0<)1-\eta_o\equiv\bar{\tilde{A}}_o^{-2}\Big/\bar{\tilde{A}}_o^2\le 1,\ \text{(Eq. (65a), [4]); } J=MN\right)$$

$$= 2\Pi^{(*)}_{coh}\cdot\left\{\left\langle a_o^2\right\rangle_{min-det}\right\},\ \text{cf. (2.6b,c)}, \tag{5.13a}$$

which last defines the minimum detectable signal (power ratio). The quantities $F_{S,V,B}$, $F_\sigma^{(m)}$ are the respective structure factors of the various reverberation components *and of the target signal* (cf. 4.7) *(all of which depend on the input signal!)*, and the quantity $\Delta\tau_m$ appearing in $\hat{t}_{m,n}$, cf. (5.11) et seq., and (5.13). We shall refer to the explicit forms of these structure factors in **B** ff.

For preformed beams we formally drop the dependence on (m) in the above (5.10)-(5.13), so that (5.13) reduces to the simpler result

$$\sigma^{(*)2}_{N\text{-coh}}\Big|_{preformed} = 2L^{(2)}N\left\{\frac{(1-\eta_o)}{\left\{F_S+F_V+F_B+\Psi_{A+G}/\bar{\tilde{A}}_o^2\right\}}\sum_{n}^{N}\frac{\overline{\left|s_o(t_n-T_o-\varepsilon_o)_{in}\right|^2}\,F_\sigma(t_n-T_o-\varepsilon_o)}{2N}\right\}. \tag{5.14}$$

The optimum threshold detection algorithm (5.3) now becomes

$$g_N(\mathbf{x})^*_{coh} = \hat{B}^*_{N\text{-coh}} + \log\mu - \sum_{n=1}^{n} l(x_n)\langle\theta_n\rangle\,,\quad \mathbf{x}=\left\{x_n=x(t_n)\right\}, \tag{5.15}$$

with

$$\sigma^{(*)2}_{N\text{-coh}} = -2\hat{B}^{(*)}_{N\text{-coh}} = \text{Eq. (5.14), etc.} \tag{5.15a}$$

B. Components of the Channel Model

We consider, again in summary form, the various channel components that we need for evaluating the detection parameters (5.13), (5.14). These are of two classes: the target structure factor (TSF), for both adaptive and preformed beams, and the different reverberation structure factors (RSFs), all of which are distinguished here by being input signal-dependent.

From (4.1), extended to include the original array elements (m), we write generally in these coherent detection cases for the TSF:

I. *TSF-adaptive beamforming*:

$$F^{(m)}_{\sigma\text{-}n}(t_n - T_o - \varepsilon_o;\ \Delta\tau_m) = \Big|\sqrt{G^1}\int\Big\langle \mathcal{A}_T(\ell)e^{-2ik_o\alpha_o\ell} \cdot\int_{-\infty}^{\infty}\Big\langle \exp\Big\{-ik_o(2\alpha_o\cdot v_d)\big(\hat{t}_n + \Delta\tau_m - \varepsilon_o - \tau\big)\Big\}\Big\rangle_{v_d} \cdot\big\langle q_L(\ell,\ t_n - T_o + \Delta\tau_m - \tau)\big\rangle s_o(\tau - \varepsilon_o)_{in} \cdot e^{i\omega_o(\tau-\varepsilon_o)}d\ell dt\Big\rangle_{\alpha_o}\Big|^2 \Big/ \Big|s_o(t_n - T_o - \varepsilon_o)_{in}\Big|^2 , \qquad (5.16)$$

with ε_o to maximize $F^{(m)}_{\sigma\text{-}n}$; $\hat{t}_n$ = Eqs. (6.10a,b) [1], for the appropriate Doppler scenario; $k_o = \omega_o/c_o$. Here $G^{(1)} = G^{(1)}(f_o)$ for these narrowband, far-field cases is given by Eq. (4.1a), and q_L is the local target kernel, (4.3). For bistatic and monostatic regimes, $2\alpha_o$, (4.2a), is given specifically by (6.14a,b), [1]; see *Figures 4.1* and *4.2*. Here ε_o is chosen to maximize the signal for these coherent cases, which usually means picking a maximum of the "carrier" component of Re $\hat{S}_{o\text{-}in}$; $\hat{S}_{o\text{-}in}$, of course, is the (complex) envelope of the input signal, as discussed in Secs. 4, 8 [1]. Finally, $\mathcal{A}_T$ is the (complex) beam pattern of the transmitter.

The relation ((5.16) for the TSF simplifies for the case of preformed beams. Thus, we have Eq. (6.17a), [1].

II. *TSF-preformed beams*:

$$F^{(m)}_{\sigma\text{-}n} \to F_{\sigma\text{-}n} = F_\sigma(t_n - T_o;\ \varepsilon_o,\ \ldots)\ ;\ \Delta\tau_m \to 0 \text{ formally},\ \mathcal{A}_T \to \mathcal{A}_{RT} \Big\} \text{ in (4.1)} . \qquad (5.17)$$

The details of (5.17) are developed in Sec. 6,[1], with various specific, elementary target models presented briefly in Sec. 7, [1].

In a similar fashion we may describe the Reverberation Structure Factors (RSFs), cf. Sec. 10.2 of [1]. We have

III. *Reverberation Structure Factors:* $F_{S,V,B}$:

We have normalized our results with a mean-square noise Ψ, (2.3), which, however, is not stationary, as in the usual treatments [1], [5], v. Thus,

$$\Psi = K_X(t_1,t_1) + \Psi_{A+G} + \Psi(t_1)\ ;\quad \Psi(S) = \text{Re}\,K_X(t_1,t_1) \equiv \hat{K}_X(t_1,t_1) \qquad (5.18)$$

from (8.4), [I], where X = reverberation process and K_X is its (complex) covariance; see Eq. (5.20). Since our signals [Sec. 8.2, [1], and *Figure 5.1*] are pulses, of finite duration $T<(<T_O)$, it is appropriate in the first-order treatment here to select the path delay $t_1 \equiv T_o + T/2 = T_o'$, namely, the midpoint of the pulse about the target location (at O_L, cf. *Figure 6.1*[1]). Accordingly, from the fact that $\Psi_S = \langle \tilde{A}_o^2 \rangle (F_S + F_V + F_B) = \hat{K}_X(T_o', T_o')$ now, we may use (3.11) to represent the reverberation structure factors, generally, by

$$F_{R=S,V,B}(T_O') = \mathrm{Re}\left\{ K_X(T_O', T_O') \Big/ \langle \tilde{A}_O^2 \rangle \right\} = \hat{K}_R \Big/ \langle \tilde{A}_O^2 \rangle \,, \tag{5.19}$$

where for these n.b. input signals $\hat{K}_R(T_O', T_O')$ is given by (3.11), with $t(=t_2) \to T_o'$ and with

$$F_S + F_V + F_B = \sum\nolimits_R \hat{K}_R(T_o', T_o') \Big/ \langle \tilde{A}_o^2 \rangle \tag{5.20}$$

to be used in (5.13), (5.14). The first term of (3.11) embodies the (usually) primary, first-order or single-scatter contributions, while the second term contains all higher scatter interactions. The signal-dependent character of $\hat{K}_R$ is at once evident, where $s_{o\text{-}in}$ here is described specifically in Section 8.2,[1] for the present applications. As we noted in Section 3.2, it is in principle possible to calculate some of the scattering functions, σ, and the cospreading functions, $\Omega_s^{(k)}$. The critical rôle of geometry appears in the structure of $\sigma_s, \Omega_s^{(\infty)}$, as expected. Equation (3.13) is an explicit example of $\sigma_s(\tau, \nu)$.

Various approaches giving explicit results for F_R are listed below, with some comments:

	Reverberation Models, $\hat{K}_R$		
	FOM Theory [8]	← *WSSUS* $F_R = S,V,B$ →	*"Classical" [10]*
n.b. f.f. N.B. s.d.	Eqs. (9.18), (9.18a)		Eq. (51): $M_{X\text{-}(X)}(\tau)$
	Eqs. (9.19), (9.21):	"short signals" ↔	Eq. (50): $M_X(\tau)$

Remarks: Volume (V), surface (S), and bottom (B):

(V) *Volume:* gauss, nongauss process

(S) *Surface:* ocean surface (gauss); nongauss at small angles, N.B.

(B) *Bottom:* nongauss; ice bottoms also.

These scatter channels are not entirely WSSUS (wide sense stationary uncorrelated scatter) channels.

C. Optimization by Choice of Signal Waveforms: Remarks

Finally, an important question here is the choice of input signal waveforms, to optimize further, or at least increase, the detection parameter $\sigma_J^{(*)}$. The reason for this is that increasing signal level alone buys little improvement in performance because of the corresponding increase in the reverberation, which is signal-dependent. Therefore, one must seek signal waveforms for a given signal energy, which because of their coherent structure vis-à-vis the reverberation, can discriminate against the latter, in effect increasing $\sigma_J^{(*)}$. In these instances the customary energy constraint (used against an additional signal-independent background noise) must be replaced by one that preserves the area under the ambiguity function of the input signal, or requires it to be some specified function of unity, subject to bounds on ν and τ, cf. (3.9), (3.10), *so that* the reverberation intensity $K_X(t_1,t_1) = \Psi_{S+V+B} = \Psi(S)$ is reduced vis-à-vis $\sum_n \overline{|s_{on}|}^2 F_o$ in (5.13), (5.14), for example. Some typical signal structures for this purpose are described in Section 8.2 of [1], along with a sketch of a formal variational procedure for maximizing the detection parameter.

6. CONCLUDING REMARKS AND NEXT STEPS

In the preceding sections we have provided a guide to, and review and overview of, the analytic methods and principal results of the author's recent approaches [1] to the treatment of the actual threshold detection of weak targets in a reverberation dominated ocean environment. The aim here has been to present this material in a logical sequence and in sufficient detail so that the reader can proceed from this work to implement the various next steps (noted in part below), which are needed in the practical application of the analysis, as well to explore and use the analytical details developed in the original study [1]. In this sense [1] is the in-depth "backup" to this paper.

Here we have summarized our results for the following elements, all of which play their significant rôle in achieving practical, near-optimal algorithms and performance for these active detection systems in typical ocean milieux (cf. *Figure 5.1*). These include

(1) Channel models, whose component processes are required in order to implement the target detection algorithms and to predict performance (Sections 2, 3);

(2) In particular, the various *Structure Factors* (cf. Section 5.2) needed for
   - A. *The target model(s)* - which here are spatially linear (cf. Section 4);
   - B. *Reverberation* - General results, for surface (S), volume (V), and bottom (B) (cf. Section 3);
   - C. *WSSUS Channels* in particular (Section 3);
   - D. Multiple scatter contributions (non-WSSUS components), Section 3;

The analytic models for these are specialized to account for the principal conditions of operation here, namely:

$$\begin{cases} \text{n.b.} \equiv \text{"narrowband" or "short" signals ;} \\ \text{N.B.} \equiv \text{"narrow - beams," usually preformed ;} \\ \text{f.f.} \equiv \text{"far - field" operation, e.g., in the Fraunhofer region ; and} \\ \text{s.d.} \equiv \text{small dopplers, a general condition ,} \end{cases}$$

with independent noise sampling and zero-gradient $(\nabla c = 0)$ propagation models.

(3) General and specific (i.e., coherent) threshold detection algorithms (cf. Section 5);

(4) Canonical waveforms and noise models, both ambient and reverberatory (cf. Sections 2-4);

(5) Performance measures, both canonical and specific to these signal-dependent situations (cf. Section 5); and

(6) Results for both adaptive and preformed beams.

Some Next Steps:

A variety of next steps is needed (also noted in [1].) We list (not necessarily in order of importance) the following:

(1) Treatment of dependent noise samples, primarily spatial [16];

(2) $(\nabla c \neq 0)$: this is the usual situation ([8], parts III, IV);

(3) Incoherent detection modes; mixed coherent and incoherent; with generalizations of the usual ambiguity function;

(4) Detailed evaluation of F_S, $F_{R=S,V,B}$, for "short signals";

(5) Experimental design - rôle of multiple scattering and measurement of departure from the WSSUS state (cf. Section 3);

(6) Determination of the surface structure functions, F_S, in detail;

(7) Adaptive arrays, "matched field" processing;

(8) Extension of the general n.b. treatment to "broadband" $(f_o/\Delta F < 2 \text{ or } 3)$ cases;

(9) Multiple "ping" integration;

(10) Comparisons of performance for different signal classes;

(11) Analytical derivation of the optimal waveform class in these signal-dependent backgrounds; and

(12) Estimation ("classification") problems in these detection environments [16].

Some additional results, and next steps, are also cited in [1], Sections 2, 2.2; Section 3.G; Section 5; and Section 7.1.

REFERENCES

[1]. D. Middleton, "Scatter Channels and Target Modeling for Active Signal Extraction in Underwater Acoustics: I. Formulation and Analytic Overview," NUSC Tech. Document TD-8991, September, 1991, Code 3314, NUSC, New London, CT 06320.

[2]. _____, "Channel Modeling and Threshold Signal Processing in Underwater Acoustics: Are Analytical Overview," IEEE J. Oceanic Eng., Volume OE-12, No. 1, January 1987, pp. 4-28.

[3]. D. Middleton, *An Introduction to Statistical Communication Theory*, McGraw-Hill (New York), 1960; Reprint Ed. 1987, Peninsula Publishing, P.O. Box 867, Los Altos, CA 94023.

[4]. R. S. Kennedy, *Fading, Dispersive Communication Channels*, John Wiley (New York), 1969.

[5]. H. L. Van Trees, *Detection, Estimation, and Modulation Theory: III, Radar/Sonar Signal Processing and Gaussian Signals in Noise*, John Wiley (New York), 1971.

[6]. D. Middleton, "Acoustic Scattering from Composite Wind-Wave Surfaces in 'Bubble Free' Régimes," IEEE J. Oceanic Engineering, Volume 14, No. 1, January, 1989, pp. 17-75.

[7]. S. M. Flatté, R. Dashen, W. H. Munk, K. M. Watson, F. Zachariasen, *Sound Transmission through a Fluctuating Ocean*, S. M. Flatté, Ed., Cambridge University Press (New York), 1979; see the Introduction.

[8]. D. Middleton, "A Statistical Theory of Reverberation and Similar First-Order Scattered Fields," Parts I, II: pp. 372-392, 393-414, IEEE Trans. Information Theory, Volume IT-13, 1967; Parts II-IV: pp. 35-67, 68-90, Volume IT-18, 1972.

[9]. _____, "Some Operational Formulations for Computational Solutions of Underwater Acoustic Scattering Problems," NUSC TD-8589, 21 November 1989, NUSC, New London, CT 06320.

[10]. D. Middleton, "Acoustic Scattering by Wind-Generated Wave Surface Solitons: A Critical Summary," *Computational Acoustics*, Volume 2, pp. 173-198, Ed., D. Lee, R. L. Sternberg, M. H. Schultz, IMACS, 1988, Elsevier (North Holland) New York.

[11]. D. Middleton and R. H. Mellen, "Experimental Evidence for a Proposed Surface Soliton Mechanism in Wind-Wave Generation and Scattering," J. Acous. Soc. Amer., **90** (2), Part 1, August, 1991, pp. 741-753.

[12]. D. Middleton, "Second-Order Non-Gaussian Probability Distributions and Their Applications to "Classical" Non Linear Processing Problems in Communication Theory," *Proc. 1986* Conference on Information Sciences and Systems", pp. 393-400, March 19-21, 1986, Princeton University, Princeton, New Jersey.

[13]. _____, "Space-Time Processing for Weak-Signal Detection in Non-Gaussian and Non-Uniform Electromagnetic Interference (EMI) Fields," Contractor Report 86-36, February, 1986, ITS/NTIA, U.S. Dept. of Commerce, 325 Broadway, Boulder, CO 80303.

[14]. _____, "Threshold Detection in Non-Gaussian Interference Environments: Exposition and Interpretation of New Results for EMC Applications," IEEE Trans. Electromagn. Compat., Volume EH-26, No. 1, pp. 19-28, February, 1989.

[15]. G. V. Trunk and S. F. George, "Detection of Targets in Non-Gaussian Sea Clutter," IEEE Trans. Aerospace and Electronic Systems, Volume AES-6, No. 5, pp. 620-628, September 1970. Also, G. V. Trunk et al, ibid., May, 1971, pp. 553-556, Volume AES-7, No. 3, and pp. 196-204, Volume AES-8, No. 2, March 1972.

[16]. D. Middleton, "Threshold Detection and Estimation in Correlated Interference," Proc. 9th Int'l. Zürich Symposium Electromagnetic Compatibility, Zürich, Switzerland, March 12-14, 1991: paper A2, pp. 7-12.